OFFICE OF NAVAL RESEARCH

Contract N00014-88K-0360
R&T Code B41C004DAR01

Technical Report No. 7

Impedance Analysis of Ionic Transport in Polypyrrole-Polyazulene Copolymer and Its Charge-Discharge Characteristics

by

K. Naoi, K. Ueyama, T.A. Osaka and W.H. Smyrl

Submitted for Publication

in

The Journal of the Electrochemical Society

Corrosion Research Center
Department of Chemical Engineering and Materials Science
221 Church St. SE
University of Minnesota
Minneapolis, MN 55455
and
Department of Applied Chemistry
Waseda University
Tokyo, Japan

June 15, 1989

SECURITY CLASSIFICATION OF THIS PAGE

REPORT DOCUMENTATION PAGE

1a. REPORT SECURITY CLASSIFICATION **Unclassified**	1b RESTRICTIVE MARKINGS
2a. SECURITY CLASSIFICATION AUTHORITY	3 DISTRIBUTION / AVAILABILITY OF REPORT
2b. DECLASSIFICATION / DOWNGRADING SCHEDULE	**Unclassified/Unlimited**
4. PERFORMING ORGANIZATION REPORT NUMBER(S) **ONR Technical Report 7**	5. MONITORING ORGANIZATION REPORT NUMBER(S)
6a. NAME OF PERFORMING ORGANIZATION **Dept. of Chem. Eng. & Mat. Sc.** **Corrosion Research Center** 6b. OFFICE SYMBOL (*If applicable*)	7a. NAME OF MONITORING ORGANIZATION **Office of Naval Research**
6c. ADDRESS (*City, State, and ZIP Code*) **University of Minnesota** **Minneapolis, MN 55455**	7b ADDRESS (*City, State, and ZIP Code*) **800 North Quincy Street** **Arlington, VA 22217-5000**
8a. NAME OF FUNDING / SPONSORING ORGANIZATION **DARPA/ONR and Gen Sekiyu R&D Assist Found** 8b OFFICE SYMBOL (*If applicable*) **Code 1113**	9. PROCUREMENT INSTRUMENT IDENTIFICATION NUMBER **Contract No. N00014-88-K-0360**
8c. ADDRESS (*City, State, and ZIP Code*) **800 North Quincy Street** **Arlington, VA 22217-5000**	10 SOURCE OF FUNDING NUMBERS PROGRAM ELEMENT NO. / PROJECT NO. / TASK NO. / WORK UNIT ACCESSION NO

11. TITLE (*Include Security Classification*)
Impedance Analysis of Ionic Transport in Polypyrrole-Polyazulene Copolymer and Its Charge-Discharge Characteristics

12. PERSONAL AUTHOR(S)
K. Naoi, K. Ueyama, T.A. Osaka and W.H. Smyrl

13a. TYPE OF REPORT	13b. TIME COVERED	14 DATE OF REPORT (*Year, Month, Day*)	15. PAGE COUNT
Technical	FROM **7/88** TO **6/89**	**89/06/15**	**25**

16. SUPPLEMENTARY NOTATION
Submitted to J. Electrochemical Society

17 COSATI CODES			18. SUBJECT TERMS (*Continue on reverse if necessary and identify by block number*)
FIELD	GROUP	SUB-GROUP	

19 ABSTRACT (*Continue on reverse if necessary and identify by block number*)

Ionic transport behavior across an electropolymerized polypyrrole/polyazulene composite film was investigated by using ac impedance analysis, and its charge-discharge characteristics were also studied. Co-electropolymerization of pyrrole and azulene was well defined and fairly stoichiometric in propylene carbonate solution. The charge capacity for the composite films, showed a remarkable increase for films around 50 to 75% of azulene monomer content, and the behavior was correlated with morphological and diffusivity changes. The charge-discharge characteristics were examined for cells with a lithium anode and various polypyrrole/polyazulene composite cathodes. Pure polypyrrole cathodes behaved exactly like a capacitor at low frequency, while pure polyazulene cathodes showed excellent rechargeable behavior with very flat discharge curves. Composite cathodes showed intermediate behavior.

20. DISTRIBUTION / AVAILABILITY OF ABSTRACT	21. ABSTRACT SECURITY CLASSIFICATION	
☒ UNCLASSIFIED/UNLIMITED ☐ SAME AS RPT ☐ OTIC USERS	**Unclassified**	
22a NAME OF RESPONSIBLE INDIVIDUAL **Boone B. Owens**	22b. TELEPHONE (*Include Area Code*) **(612) 625-1332**	22c. OFFICE SYMBOL

DD FORM 1473, 84 MAR — 83 APR edition may be used until exhausted. All other editions are obsolete.

SECURITY CLASSIFICATION OF THIS PAGE

Unclassified

Impedance Analysis of Ionic Transport in Polypyrrole-Polyazulene Copolymer and Its Charge-Discharge Characteristics

Katsuhiko Naoi,*,+,++ Ken-ichi Ueyama and Tetsuya Osaka*
Department of Applied Chemistry,
School of Science and Engineering, Waseda University,
3-4-1 Okubo, Shinjuku, Tokyo 160, JAPAN

William H. Smyrl*
Department of Chemical Engineering and Materials Science,
University of Minnesota,
221 Church St SE, Minneapolis, Minnesota 55455, U.S.A.

ABSTRACT

Ionic transport behavior across an electropolymerized polypyrrole/polyazulene composite film was investigated by using ac impedance analysis, and its charge-discharge characteristics were also studied. Co-electropolymerization of pyrrole and azulene was well defined and fairly stoichiometric in propylene carbonate solution. The charge capacity for the composite films, showed a remarkable increase for films around 50 to 75% of azulene monomer content, and the behavior was correlated with morphological and diffusivity changes. The charge-discharge characteristics were examined for cells with a lithium anode and various polypyrrole/polyazulene composite cathodes. Pure polypyrrole cathodes behaved exactly like a capacitor at low frequency, while pure polyazulene cathodes showed excellent rechargeable behavior with very flat discharge curves. Composite cathodes showed intermediate behavior.

Electropolymerization has been gathering growing interest recently, as an elegant new way of preparing conducting polymer films, eg., polyaniline[1-7], polypyr-

role(PPy)[8-14]. The process is fairly stoichiometric and simple without using the strong oxidizing agents like halogens or AsF_6 that are used in conventional chemical processes. With the electrochemical technique, various qualities of polymeric films can be prepared by simple electro-oxidation of monomers with varied polymerization factors. The factors include, for example, kind of monomer, electrolysis mode(controlled potential[11], controlled current[3,11]), electrolyte anion[11,12], and passed charge(thickness)[12]. By choosing appropriate conditions for these factors, we can deliberately design the structure/morphology and electrochemical redox properties of resulting films so as to tailor them to specific applications, such as energy storage or microelectronics.

The electropolymerization method is also a powerful means to prepare random co-polymerized or composite polymers by mixing different kinds of monomers in the starting polymerization solution. In general, co-electropolymerization of different monomers gives amorphous films with little interactions among monomers[16]. The resulting film is then a polymer composite in the sense of its elemental composition. However, in some cases, it shows noticeable changes in morphology compared to the individual pure polymers. The morphological changes result in changes(acceleration/retardation) in ionic transport behavior across the film. The ionic transport behavior is especially important for controlling the rate capability of energy storage devic[illegible]2].

Among conducting polymers, polypyrrole-based composite films are the most extensively studied. Co-polymerization of pyrrole has been reported with other kinds of monomers such as thiophene[15], azulene[16], and N-substituted pyrrole with methyl-[17,18,19] or phenyl-groups[19,20]. One of the best example is the co-polymerization of pyrrole and azulene which shows fairly stoichiometric and reproducible polymerization behavior. Since pyrrole and azulene show similar electro-reactivity(oxidation potentials) and polymerization scheme(α-α' linkage at 5-membered rings)[21-24], they mix with each other fairly well during electro-polymerization to form a uniform composite film. Electro-polymerized polyazulene(PAz) shows moderately high conductivities(10^{-2}-10^{0} Ω^{-1} cm-

^{1})[21] in the dry state, and a bulky morphology that depends greatly on the kind of co-existing anion[23]. Also, PAz film is an effective cathode material in lithium cells because it has a high redox potential and high switching reversibility[22,24].

The combination of PPy and PAz is a kind of composite of bulky(azulene) and less bulky(pyrrole) monomers. The insertion of the bulky azulene group into a PPy matrix causes the PPy/PAz composite film to look much rougher than PPy itself, and to show various packing structures that depend on the pyrrole/azulene monomer ratio in the film. This kind of rough film is specifically suitable for application as an energy-storage material like a redox capacitor[28], or rechargeable battery which can tolerate high-rate charging/discharging.

So far, the PPy/PAz film has received only limited attention except for structural analysis by IR spectroscopy[16]. The authors have investigated the ionic transport phenomena across the PPy/PAz composite film using the same techniques that have been used earlier for polyvinylferrocene(PVF)[27], i.e., by cyclic voltammetry and AC impedance spectroscopy[25-27]. The emphasis of the present paper is to report the variations in redox capacity and diffusivity of anions for different PPy/PAz composite films, and how these properties are related to the observed morphology by SEM.

Experimental

Chemicals and Solutions

Reagent grade $LiClO_4$ and propylene carbonate(PC) were used as the electrolyte salt and solvent, respectively. PC was used after purification by percolating through activated alumina. Water in the PC was removed by adding molecular sieves to it and letting it stand for a few days until use[11,12,18,24]. Highest grades of azulene(Az) and pyrrole(Py) monomers were used as obtained without further purification.

PC solutions(degassed with Ar gas) containing 0.1 mol dm^{-3} $LiClO_4$ plus Py and/or Az monomers were used for the preparation of polymer films. The total concentration of Py and Az monomers were kept constant(0.05 mol dm^{-3}). Monomer ratios for the five different solutions are shown in Tab. 1. In this table, the solutions of Az%=0 and 100 correspond to 100% Py and 100% Az solutions, respectively.

Cyclic voltammetry, impedance spectroscopy, and charge/discharge performance tests were carried out in 1.0 mol dm^{-3} $LiClO_4$/PC solution.

Film Preparation

Polypyrrole/polyazulene(PPy/PAz) composite films were prepared on Pt plate(0.283 cm^{-2}) in the PC solutions mentioned above using the cell assembly described elsewhere[11,12,18,24]. Electropolymerization was performed at a constant potential of 4.2 V(*vs.* Li/Li^+ in the same solution), at which the oxidation of both Py and Az occurs at almost equal electroreactivity under diffusion control[16]. Total deposition amounts of the polymers were determined by monitoring the charge consumed during electropolymerization.

Free standing films, prepared by the passage of the same amount of charge(2 C cm^{-2}), were inspected by scanning electron microscopy(SEM).

Electrochemical Measurements

Cyclic voltammetry was employed for surveying both electropolymerization behavior at a scanned potential(10 mV s^{-1}) and redox(doping/undoping) processes at grown polymer films. As for impedance measurements, ac voltage signal(maximum amplitude = 5 mV peak to peak) superimposed on dc bias was applied to the cell as a perturbation, and the response current signal was analyzed using FFT techniques. The range of frequencies was 5 mHz to 100 kHz. Li/1.0 mol dm^{-3} $LiClO_4$-PC/(PPy/PAz) cells were assembled with a (PPy/PAz)/Pt cathode and Li/Ni-mesh anode in a small container purged with dry and pure Ar gas. Charge-discharge tests were conducted at constant current densities(0.1 - 1.4 mA cm^{-2}). Discharge of the cells was terminated when the cell voltage reached 2.5 V. All the results of cyclic voltammograms and charge-discharge curves in this work were obtained after being stabilized several cycles in ambient temperature(25°C).

Results and Discussion

Polymerization Curves

Figure 1 shows consecutive cyclic voltammograms for the polymerization of PPy, PAz and their composite films at a Pt electrode in $LiClO_4$ solutions containing a) 100 % Py monomer(Az%=0), b) Py and Az monomer(Az%=50) and c) 100 % Az monomer(Az%=100), respectively. In terms of the polymerization behavior at the first scan, each voltammogram has almost the same onset oxidation potential(ca. 3.6 V) and shows a limiting current beyond ca. 4.1 V for 100% pyrrole, and ca. 4.2 V for 100% azulene solutions. Azulene monomer shows a wider limiting current region than pyrrole, which is consistent with the results obtained by Burzynski et al.[16]. However, the rate of monomer feed would be more or less the same in this diffusion controlled region of over ca. 4.2 V. Therefore, the polymerization potential for the following results was set at 4.2 V. In the solution of Py/Az=50/50, intermediate behavior of these two monomers was observed. No cathodic currents were observed for the first scan except for that due to undoping anions. This indicates that both Py and Az monomers were oxidized to form radical cations to yield polymeric films, and the films do not decompose cathodically in this range.

From the second scan, anodic and/or cathodic currents in the voltammograms grow in each succeeding cycle(indicated by arrows). The current involves oxidation of monomers(radical cation formation) at over 3.6 V, as well as the oxidation of polymer films themselves on the substrate. The oxidation/reduction process of polymer films has concurrent anion doping/undoping at their active sites. The interesting observation is that continuous current growth occurs for azulene and pyrrole/azulene solutions, but the 100% pyrrole solution shows saturation in the oxidation region(over *ca.* 4.0V). The former two cases suggest that electroactive conducting polymers are continuously deposited layer after layer from the solutions. It is likely that the diffusivity of dopants limits the current for polymer growth when the polymerization speed is very high and the concentration gradient becomes very steep across the interface between polymer film and electrolyte. Because PPy films are more compact than PAz films[24], the film deposition for PPy shows saturation, but PAz deposit in the conditions investigated here.

Elemental Analysis of Composite Films

Table 2 shows the results for the elemental analysis of PPy, PAz and PPy/PAz composite films prepared from PC solutions of various Az content at 4.2 V *vs.* Li/Li^+. The numbers X and Y correspond to the monomer ratios of Py and Az found, respectively, in composite polymer films$[-(Py)_x-(Az)_y]_n$. From this table, it can be seen that the films contain exactly the same ratios of Py and Az monomers as in the starting solutions. Hence the polymerization occurred at almost the same efficiencies for the two monomers at the potential of 4.2V.

Cyclic Voltammograms for PPy/PAz Composite Films

Figure 2a) shows typical cyclic voltammograms at 5 mV s^{-1} for PPy , PPy/PAz and PAz films deposited from various PC solutions of Az%=0, 25, 50, 75 and 100%. In these voltammograms, the anodic and cathodic currents correspond to anion doping and undoping processes accompanied by the oxidation and reduction of the film itself. The voltammograms were repeatedly cycled without any decay of current, meaning that all the films were chemically stable and reproducible in the potential range between 2.5 and 3.8 V.

The voltammogram of each PPy/PAz film has well-defined single redox peaks, and the redox potential($\approx E_{pac} = \frac{E_{pa}+E_{pc}}{2}$) increases linearly in proportion to Az% in the film as seen in Fig. 2b), where E_{pa} and E_{ac} are the potentials of anodic and cathodic peaks, respectively. The relationship between E_{pac} and Az% suggests that the PPy/PAz films prepared are not simple mixtures of PPy and PAz but completely random copolymers whose electrochemical properties are intermediate of the pure polymers[17,18].

Since all the voltammograms were obtained at a scan rate of 5 mV s^{-1}, the over-all electrode process was quasi-stationary, controlled mainly by the electron exchange reaction, but still partly controlled by ionic transport within the bulk of the films. The detected anodization or cathodization change reflected the effective number of active sites associated with the faradaic reaction at the time scale of the measurement. As the Az% was increased, the oxidation charge(Q_a) of the films became larger, *i.e.*, the total number of active sites participating in redox reaction became larger with an increase in Az% in the composite film. However, the value of Qa did not vary linearly as a function of Az%, instead the value showed an increase from 50 to 75% as seen in Fig. 2b). This implies that around this value of Az%, there was some drastic structural or morphological change of the composite film.

The scan-rate dependence of the cyclic voltammograms can be summarized as in the manner described previously[11,12]. The anodic current peaks(i_{pa}) for PPy, PAz and PPy/PAz films were plotted against the scan rate(v) on a logarithmic scale, the plot was linear with a slope, x, in the scan rate rage: 5 to 50 mV s^{-1}. Therefore, the simple relationship between i_{pa} and scan rate can be written as follows;

$$i_{pa} \propto v^x \qquad [1]$$

The value of x ($0.5 < x < 1.0$) gives information about the rate-determining process of over-all redox reaction at the polymer film electrode. So, the x value found for each film was plotted against Az% for various PPy/PAz composite films, and is shown in Fig. 3. The dashed lines at x=0.5 and 1.0 correspond to a diffusion-controlled and reaction-controlled processes, respectively. The x value shows a gradual increase from Az%=0 to 50 and attains saturation above Az%=50. This means that the electrode process becomes limited by charge injection with an increase in Az%, and ionic transport in the film is fast enough to maintain electroneutrality above Az%=50. The value of ΔE_p(peak separation potential) shows exactly the mirror image of the curve of x value, indicating that PPy/PAz films lose the ability to switch reversibility below 50% in correspondence with the change in limiting process. These two observations indicate that switching reversibility is controlled by the ionic transport of dopants. The most appreciable change in D value is observed at Az%=25-50, which is evidently consistent with the relationship between x vs. Az%. Thus, the enhancement of the diffusivity of anions is considered to be closely related to the rate-determining step of the electrode reaction. However, the C_L variation against Az% seems somewhat different from that of diffusion coefficient. Namely, the most noticeable change occurs at Az%=30-45. The C_L variation is more likely to depend on the morphological change observed in Fig.7 which is described later. This is reasonable because the deferential capacity is very sensitive to the active surface area, and the change in this number can change most likely when the morphological change at polymer surface is observed. The behavior of D and C_L values against Az% correlates to that in Fig.9.

Impedance Analysis and Estimation of Diffusion Coefficient(D) and Capacity Value(C_L)

In order to analyze the details of kinetic and diffusion processes across the PPy/PAz films as a function of Az%, impedance spectroscopy were measured. The potential dependence

of the D and C_L values shows a peak at around E_{pac} in the cyclic voltammogram for each film with different Az% film[25]. So, the impedance spectra at around anodic peak potential are compared. Figure 4 b) shows typical Cole-Cole plots for PPy/PAz films(prepared with the same charge of 1 C cm^{-2}) at the potential of each anodic peak potential of the cyclic voltammogram. These impedance spectra show the behavior typical of thin redox and electronically conductive polymer films(like PVF) as shown in Fig. 4a) [26,27]. Namely, at high frequencies(region A), charge transfer domination is observed with a semi-circle and, at lower frequencies(region B), diffusion of the anion in the polymer film dominates the impedance results. Finally at the lowest frequency(region C), the finite film thickness limits the extent of diffusion behavior, and the locus rises vertically, owing to the saturation of resistance and capacitance(C_L) components.

In the diffusion controlled region, where the impedance phase angle is $\frac{\pi}{4}$, the magnitude of the impedance is given by Eq.[2]

$$Z = \frac{C_L * L}{\sqrt{D * \omega}} \qquad [2]$$

where C_L, D, and L are the low frequency redox capacitance, diffusion coefficient and the polymer film thickness, respectively. Values of C_L were estimated from the low frequency impedance data (charge saturation region: $\omega << \frac{L^2}{D}$). In this range, the phase angle approached $\frac{\pi}{2}$ and C_L was calculated using Eq.[3].

$$\frac{1}{C_L} = \frac{d(-Z_i)}{d(\omega^{-1})} \qquad [3]$$

At very low frequencies(< *ca.* 30 mHz) in Fig. 4b), the locus for each film becomes vertical, and plots of $-Z_i$ *vs.* $\frac{1}{\omega}$ become linear as shown in Fig. 5. From the slope of the curves in Fig.5, the redox capacitance (C_L) of each film was calculated by using Eq. [3].

At intermediate frequencies(*ca.* 40 mHz < f < 210 mHz), each locus was linear with unit slope. In this region, a plot of Z *vs.* $\frac{1}{\sqrt{\omega}}$ showed a straight line as indicated with Eq.[2].

By adopting the results of Fig.5 to Eq.[2] using C_L values, values of the diffusion coefficient(D) were obtained.

In Fig. 6, the values of D and C_L are plotted against Az% for each PPy/PAz film. The obtained D values($1.0 - 7.5 \times 10^{-8}$ cm^2 s^{-1}) are in reasonable agreement with those estimated from pulse measurements[12]. The D value depended on Az% non-linearly, but jumped in the region between Az%=25 and 50 by approximately a factor of 5. This change is unexpected in view of the uniform increase in Az% in the PPy/PAz composite film which was found by elemental analysis. Above Az%=50, the D values approaches to saturation values, indicating that the diffusion attains a limiting stage(*ca.* 7.0×10^{-8} cm^2 s^{-1}) and that the structure becomes open enough to allow dopants to move smoothly in and out of the films.

The redox capacity(C_L) becomes larger as Az% increases above Az%=50. Compared to the change in D, the extent of the change in C_L($0.5 - 1.2 \times 10^{-1}$ F) is smaller and occurs at higher Az% values. The increase of C_L could be associated with the volumetric change of films caused by the incorporation of bulky azulene into the PPy matrix. This is very similar to the behavior of Q_a estimated from the cyclic voltammograms at slow scan rates. Previous reports have discussed purely capacitive behavior of polymer films at low frequencies[27,28]. Considering the above, surface roughness did not appear to change appreciably against Az% value since the ratio(Q_a/C_L) was constant against Az% in the whole range.

Morphology of Composite Films

The lower diffusion rate at low Az% may be related to the change of film morphology. In order to test this possibility, the film structures of PPy, PAz and PPy/PAz films were observed with SEM. The SEM micrographs(side views) of PPy, PAz and two PPy/PAz films(Az%= 25,50) are shown in Fig.7. Pure PPy and even PPy/PAz (Az%=25) films shows very smooth and compact structure, suggesting that polymer grows equally in every direction. On the other hand, pure PAz and PPy/PAz(Az%=50) films shows rough and perpendicularly oriented structure. This means that the incorporation PPy into bulky PAz matrix more than 50% makes the morphology somehow oriented to be like columns. The orientation of the polymer film makes more space for the flux of anion dope/undope into/out of polymer films, and leads to an enhancement of anion diffusivity(D value). The behavior(acceleration of diffusivity of anions and structure orientation) is very similar to the observation for the NBR-modified PPy films[12]. The orientation of polymer films also result in the noticeable variation of film

thickness. The thickness of these four films was estimated to be *ca.* 10 μm for both PAz and PPy/PAz(Az%=50) films, and *ca.* 6 μm for both PPy and PPy/PAz(Az%=25) films. A remarkable change in the thickness values occurred between the films of Az%=25 and 50, *i.e.*, the thickness of PAz and PPy/PAz(Az%=50) are almost twice those of PPy and PPy/PAz(Az%=25).

Charge-Discharge Characteristics of Li/LiClO$_4$(PC)/(PPy/PAz) Cells

Figure 8 shows a typical comparison of the charge-discharge curves for the two electrode cells with lithium and various PPy/PAz films, all of which were formed by the passage of 1 C cm^{-2}. Each cell was charged to 90 mC cm^{-2} at 0.2 mA cm^{-2}. The coulombic efficiencies and the average discharge voltages were calculated as follows: 94%, 3.06 V(PPy); 98%, 3.09 V(Az%=25); 100%, 3.15 V(Az%=50); 100%, 3.19V(Az%=75); 100%, 3.24 V(PAz). A striking difference was observed in the shape of discharge curves, *i.e.*, the discharge voltage became flatter and higher with an increase in Az%. In other words, 100% PPy behaved more like a pure capacitor with the linear increase/decrease in the charge/discharge curves, while 100% PAz had a flat discharge. The latter behavior is due to the higher diffusivity and higher redox potential of pure PAz(D=7.5 x 10^{-8} cm^2 s^{-1}; E_{pac}=*ca.* 3.05V) compared to that of pure PPy(D=1.0 x 10^{-8} cm^2 s^{-1}; E_{pac}=*ca.* 3.35V). The pure PAz cathode shows high capacity(low angle for V *vs.* t curve), but PPy shows a completely linear behavior in Fig.8. Higher capacity value for the pure PAz film is attributed to higher electroactivity of PAz relative to PPy because the capacity value is closely associated with the faradaic reaction itself[28]. The linear charge-discharge behavior observed for pure PPy can be explained by an ideal polarization at PPy cathode at this rate of charging and/or discharging. In other words, rate of measurement is too fast for dopants to penetrate deep into the PPy regime, but just accumulate charges at the polymer/electrolyte interface just like an ideally polarizable electrode. This explanation is likely because PPy cathodes show much flatter charge/discharge characteristics at slower rates than 0.2 mA cm^{-2}[12]. However, for such kind of films, the charging is limited up to a certain voltage because of an excessive polarization of the cell over 4.5 V at which solvents start to decompose.

The charge-discharge characteristics were further checked as a function of a) depth of charge and b) charge-discharge rate as shown in Fig. 9. Figure 9 a) shows the doping charge dependence on coulombic efficiency(η) at 0.2 mA cm^{-2}. The cell with higher Az% composite

film could be charged up to 210 mC cm^{-2} keeping more than 90% of charge retention. The charge capacity was appreciably smaller below Az%=50. At smaller Az%, the loss of the charges is more likely to be used for the polarization and/or accumulation of charges at the cathode surfaces because of the compact film morphology and therefore the slow diffusion of ions within the bulk of film. This is why the pure PPy cathode behaves more like a pure capacitor.

The rate capability of these cells were examined by varying the current density during the charge/discharge cycles. For example, the PPy/PAz cathodes containing more than Az%=50 keeps more than 90% of coulombic efficiency up to 1.0 mA cm^{-2}. On the other hand, the cathode films containing below Az%=25 show the same coulombic efficiency only at slow rates of less than 0.4 mA cm^{-2}. This means that the difference in the value of diffusion coefficient directly reflects the rate capability of these cells. For example, the ratio of the rate tolerance (PAz/PPy=1.4/0.2 =7) at η=*ca.* 92% would correspond to the ratio of diffusion coefficients(PAz/PPy=7.5 x 10^{-8} /1.0 x 10^{-8} =7.5).

Conclusions

The impedance analysis used for PVF in our previous work[27], has been adopted to co-electropolymerized PPy/PAz films. From cyclic voltammograms, the redox potential for composite films shifted linearly to more positive values with an increase in azulene content[Az%] in the films. The oxidation charge, Q_a, of active sites showed a remarkable increase for films with more than 50 to 75% of azulene monomers. From the ac impedance analysis, the diffusion coefficient, D, of dopant(ClO_4^-) and redox capacity, C_L, were estimated. Low values of D caused the electrode process to change from charge-transfer limiting to diffusion limiting process at Az%= 25 to 50% and lower. A noticeable change in C_L was observed around Az%=50 to 75%, in the same range where the morphology changed from compact to rougher condition.

The charge-discharge characteristics were examined for two electrode systems with lithium anode and PPy, PAz and various PPy/PAz composite cathodes. 100% PPy cathodes showed pure capacity-like charge and discharge. On the other hand, 100% PAz cathode showed very flat discharge behavior. Composite films are intermediate in behavior. A bulky PPy/PAz composite film at high Az% value tolerated high current-density charging/discharging.

Fig.9a) suggests that an appreciable increase in C_L value(at Az%=50-75) corresponds to higher doping level or higher energy density of the composite films. The enhancement of diffusivity(at Az%=25-50) leads to a higher rate capability or higher power density as shown in Fig.9b).

Acknowledgement

The authors would like to acknowledge the financial support from the Darpa/ONR and the General Sekiyu Res. & Dev. Encouragement & Assistance Foundation.

References

1) A. F. Diaz and J. A. Logan, *J. Electroanal. Chem.*, **111**, 111 (1980).

2) A. G. MacDiarmid, S-L Mu, N. L. D. Somasiri and W. Wu, *Mol. Cryst. Liq. Cryst.*, **121**, 187 (1985).

3) K. Abe, F. Goto, K. Okabayashi, T. Yoshida and H. Morimoto, The 27th Battery Symposium of Japan in Osaka, p.201 (1986); M. Ogawa, T. Fuse, T. Kita, T. Kawagoe and T. Matsunaga, *ibid.*, p.197 (1986).

4) A. Kitani, M. Kaya and K. Sasaki, *J. Electrochem. Soc.*, **133**, 1069 (1986).

5) G. C. Farrington, B. Scrosati, D. Frydrych and J. DeNuzzio, *ibid.*, **131**, 7 (1984).

6) E. M. Genies and C. Tsintavis, *J. Electroanal. Chem.*, **195**, 109 (1986).

7) H. Sakai, K. Naoi, T. Hirabayashi and T. Osaka, *Denki Kagaku*, **54**, 516 (1986).

8) A. F. Diaz, J. L. Castillo, J. A. Logan, and W. Y. Lee, *J. Electroanal. Chem.*, **129**, 115 (1981).

9) E. M. Genies and J. M. Pernaut, *J. Electroanal. Chem.*, **191**, 111 (1985).

10) A. Mohammadi, O. Inganaes and I. Lundstroem, *J. Electrochem. Soc.*, **133**, 947 (1986).

11) H. Sakai, K. Naoi, T. Hirabayashi and T. Osaka, *Denki Kagaku*, **54**, 75 (1986);

T. Osaka, K. Naoi, H. Sakai and S. Ogano, *J. Electrochem. Soc.*, **134**, 285 (1987).

12) T. Osaka, K. Naoi, S. Ogano and S. Nakamura, *Chem. Lett.*, **1986**, 1687; K. Naoi and T. Osaka, *J. Electrochem. Soc.*, **134**, 2479 (1987); T. Osaka, K. Naoi, S. Ogano and S. Nakamura, *J. Electrochem. Soc.*, **134**, 2096 (1987).

13) J. Bargon, S. Mohmand and R. J. Waltman, *Mol. Cryst. Liq. Cryst.*, **93**, 279 (1983).

14) R. J. Waltman, A. F. Diaz and J. Bargon, *J. Electrochem. Soc.*, **131**, 1452 (1984).

15) O. Inganaes, B. Liedberg and W. Chang-ru, *Synth. Met.*, **11**, 239 (1985).

16) R. Burzynski, P. N. Prasad, S. Bruckenstein and J. W. Sharkey, *Synth. Met.*, **11**, 293 (1985).

17) K. K. Kanazawa, A. F. Diaz, M. T. Krounbi and G. B. Street, *Synth. Met.*, **4**, 119 (1981).

18) K. Naoi, T. Hirabayashi, I. Tsubota and T. Osaka, *Bull. Chem. Soc. Jpn.*, **60**, 1213 (1987).

19) J. R. Reynolds, P. A. Poropatic and R. L. Toyooka, *Synth. Met.*, **18**, 95 (1987).

20) M. V. Rosenthal, T. A. Skotheim, A. Melo, M. I. Florit and M. Salmon, *J. Electroanal. Chem.*, **185**, 297 (1985).

21) J. Bargon, S. Mohmand and R. J. Waltman, *Mol. Cryst. Liq. Cryst.*, **93**, 279 (1983).

22) R. J. Waltman, A. F. Diaz and J. Bargon, *J. Electrochem. Soc.*, **131**, 1452 (1984).

23) G. Tourillon and F. Garnier, *J. Electroanal. Chem.*, **135**, 173 (1982).

24) T. Hirabayashi, K. Naoi and T. Osaka, *J. Electrochem. Soc.*, **134**, 750 (1987).

25) T. Osaka and K. Naoi, Unpublished data.

26) C. Ho, I. D. Raistrick and R. A. Huggins, *J. Electrochem. Soc.*, **127**, 343 (1980).

27) T. B. Hunter, P. S. Tyler, W. H. Smyrl and H. S. White, *J. Electrochem. Soc.*, **134**, 2198 (1987).

28) J. Tanguy, N. Mermilloid and M. Hoclet, *J. Electrochem. Soc.*, **134**, 795 (1987).

Tab.1 Composition of solutions at electropolymerization

	Solutions	Azulene content [mol dm^{-3}]	Pyrrole content [mol dm^{-3}]
A;	Az%= 0	0.0000	0.0500
B;	Az%= 25	0.0125	0.0375
C;	Az%= 50	0.0250	0.0250
D;	Az%= 75	0.0375	0.0125
E;	Az%=100	0.0500	0.0000

Tab.2 Elemental analysis of PPy-PAz composite films

	Solution	Composition of C H N	Monomer ratio in Composite Film Pyrrole : Azulene
A;	Az%= 0	$C_{0.49}H_{0.39}N_{0.12}$	0 : 100
B;	Az%= 25	$C_{0.54}H_{0.39}N_{0.07}$	25 : 75
C;	Az%= 50	$C_{0.57}H_{0.39}N_{0.04}$	50 : 50
D;	Az%= 75	$C_{0.60}H_{0.38}N_{0.02}$	75 : 25
E;	Az%=100	$C_{0.61}H_{0.39}$	100 : 0

Figure captions

Fig. 1 Cyclic voltammograms for the co-polymerization of Py/Az monomers in various Py/Az solutions at a scan rate of 10 mV s^{-1}.

Fig. 2 a) Cyclic voltammograms for PPy/PAz composite polymers(prepared by passing charge of 1 C cm^{-2}) at a scan rate of 5 mV s^{-1}.
b) Dependence of Az% on redox potential(E_{pac}) and oxidation charge(Q_a) estimated from the voltammograms in a).

Fig. 3 Correlation of x and ΔE_p for PPy/PAz composite films(1 C cm^{-2}) against Az%.

Fig.4 a) Ideal impedance behavior for redox polymer film. b) Cole-Cole plots for various PPy/PAz composite films(1 C cm^{-2}) at each anodic peak potentials.

Fig.5 $-Z_i$ *vs.* $\frac{1}{\omega}$ plots for various PPy/PAz composite films(1 C cm^{-2}).

Fig.6 Correlation of diffusion coefficient(D) and redox capacitance(C_L) for various PPy/PAz composite films(1 C cm^{-2}) against Az%.

Fig.7 SEM micrographs of the cross sections of various PPy/PAz(2 C cm^{-2}) composite films.

Fig.8 Charge-discharge curves for Li/1.0 mol dm^{-3} $LiClO_4$(PC)/(PPy/PAz(1 C cm^{-2})) cells. Chrarge depth= 90 mC cm^{-2}; Current density=0.2 mA cm^{-2}.

Fig.9 Coulombic-efficiency for charge-discharge curves in Fig.8.
a) Dependence of charge depth in terms of doping charge;
Current density=0.2 mA cm^{-2}.
b) Dependence of charge/discharge current density; Charge depth= 90 mC cm^{-2}.

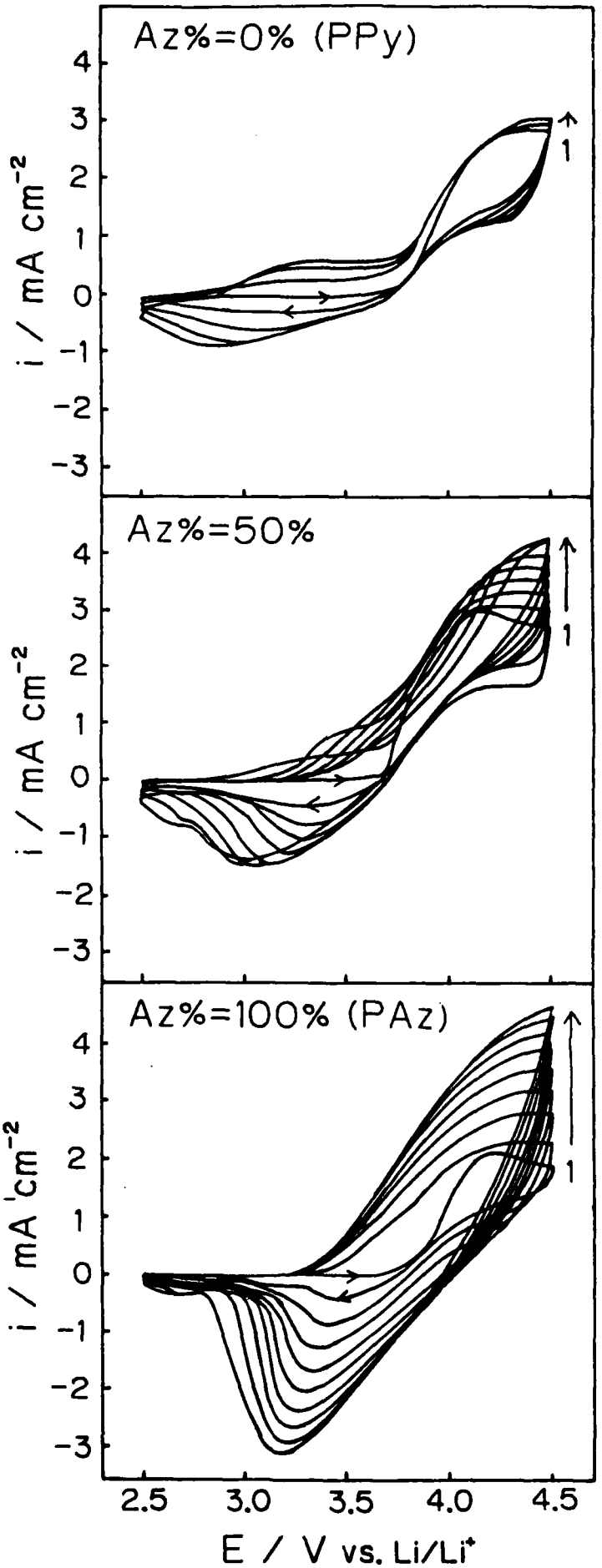

Fig 1

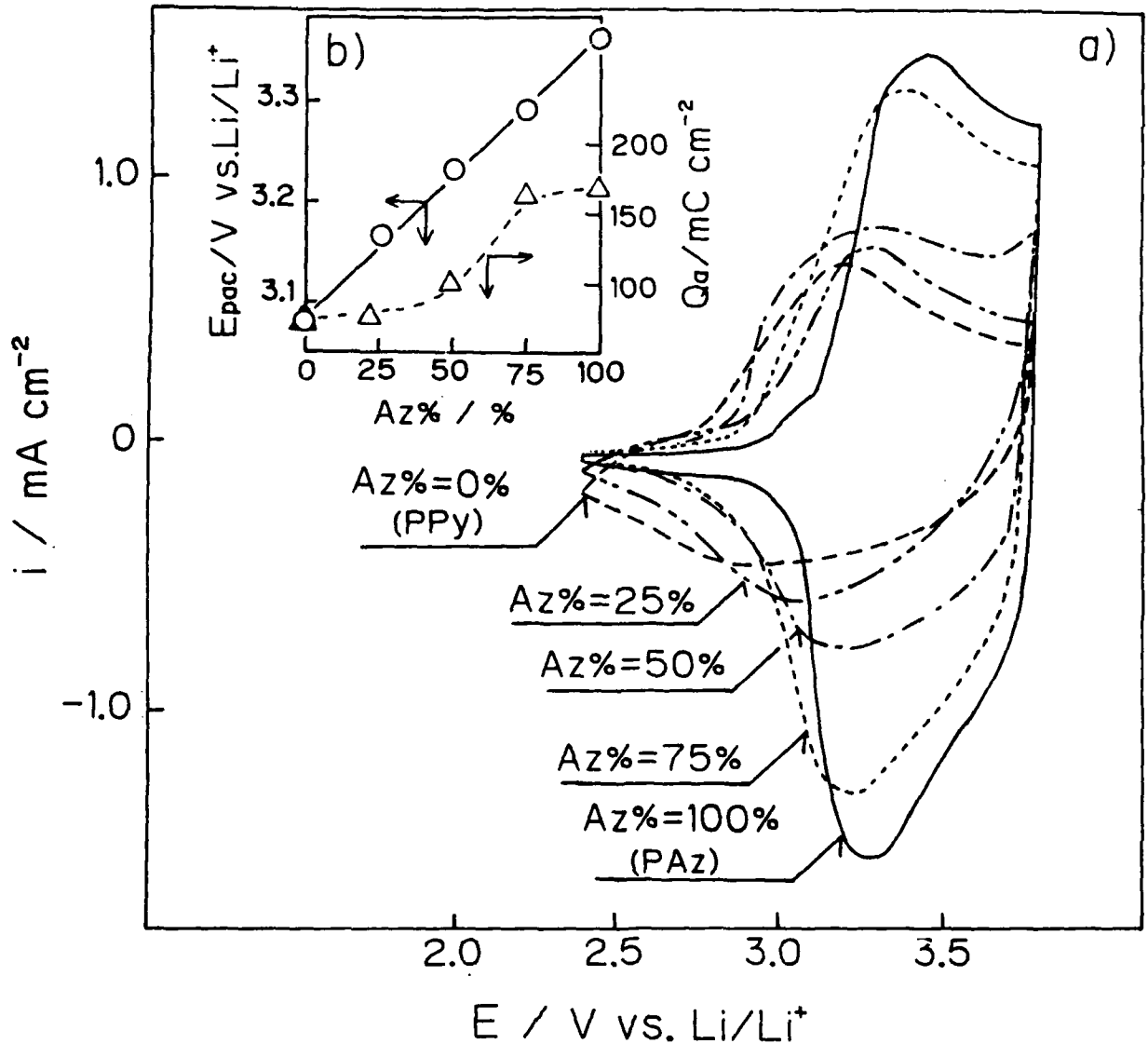
a)
b)
i / mA cm^{-2}
E / V vs. Li/Li$^+$
1.0
0
-1.0
2.0
2.5
3.0
3.5
Az%=0%
(PPy)
Az%=25%
Az%=50%
Az%=75%
Az%=100%
(PAz)
E_{pac}/V vs.Li/Li$^+$
Q_a/mC cm^{-2}
Az% / %
3.3
3.2
3.1
200
150
100
0
25
50
75
100

Fig -

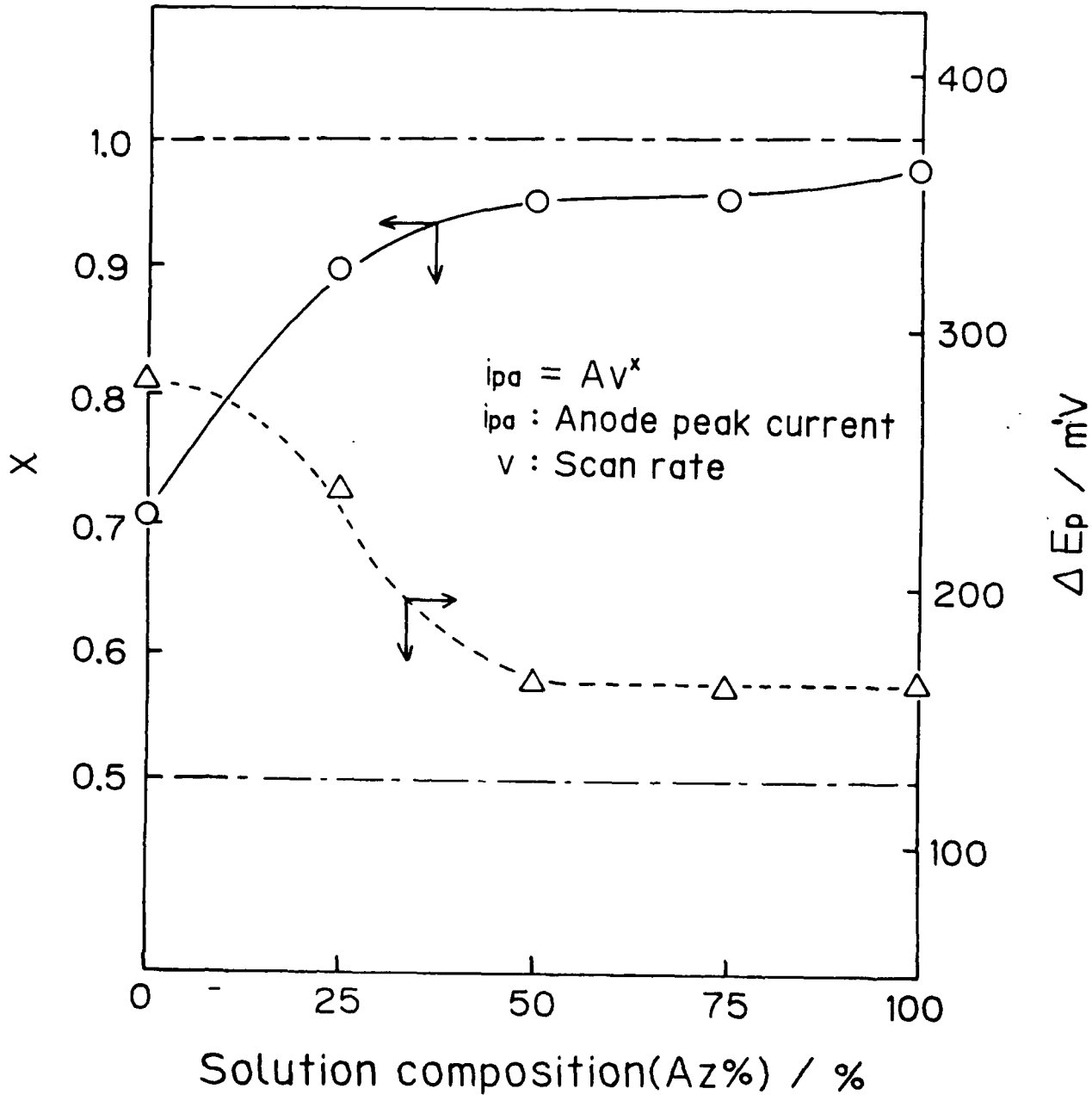
1.0
0.9
0.8
0.7
0.6
0.5
x
400
300
200
100
ΔEp / mV
ipa = Av^x
ipa : Anode peak current
v : Scan rate
0
25
50
75
100
Solution composition(Az%) / %

1/9 =

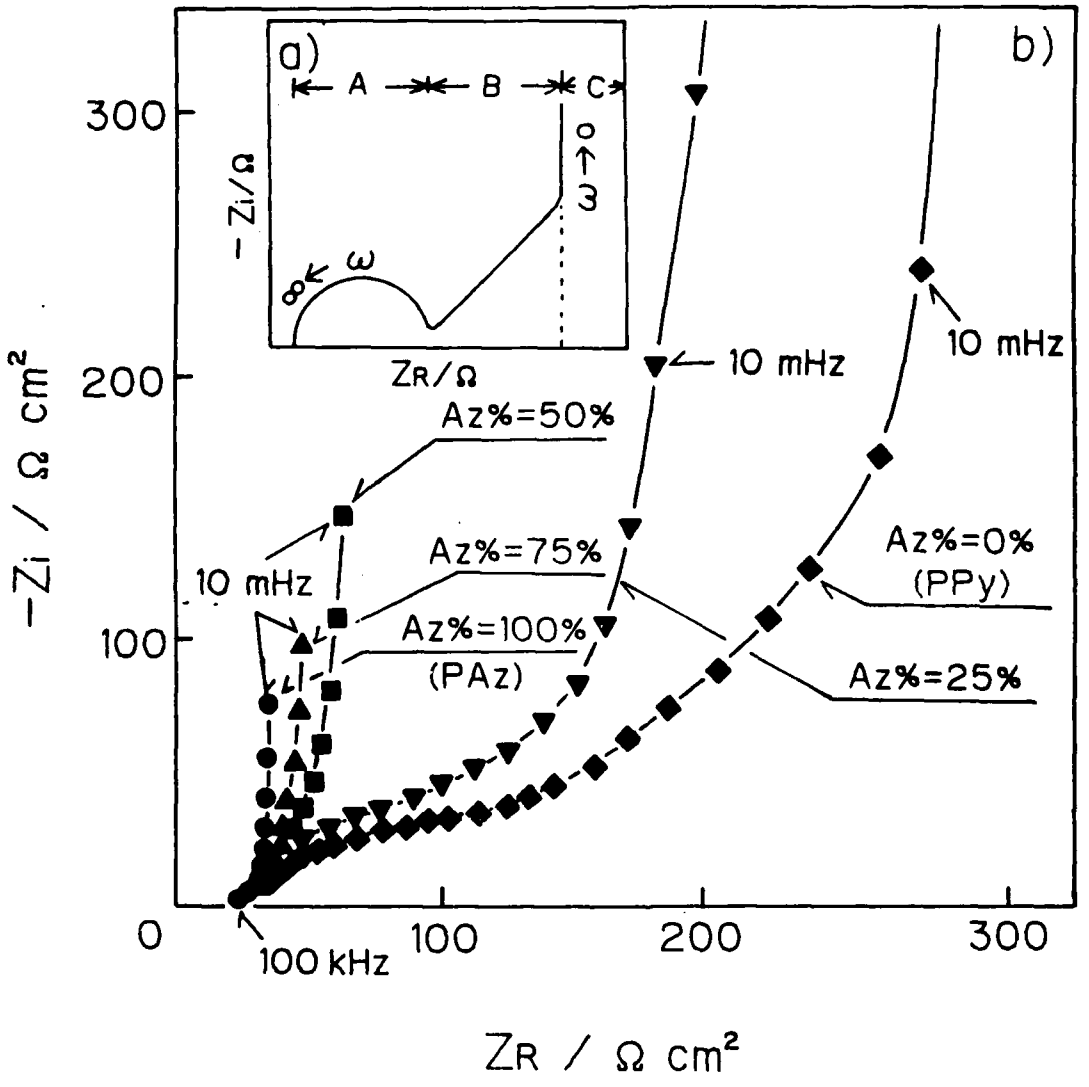
a)
A
B
C
-Zi/Ω
0
3
ω
ZR/Ω
b)
10 mHz
10 mHz
Az%=50%
10 mHz
Az%=75%
Az%=0%
(PPy)
Az%=100%
(PAz)
Az%=25%
300
200
100
0
100
200
300
100 kHz
-Zi / Ω cm²
ZR / Ω cm²

Fig. 4

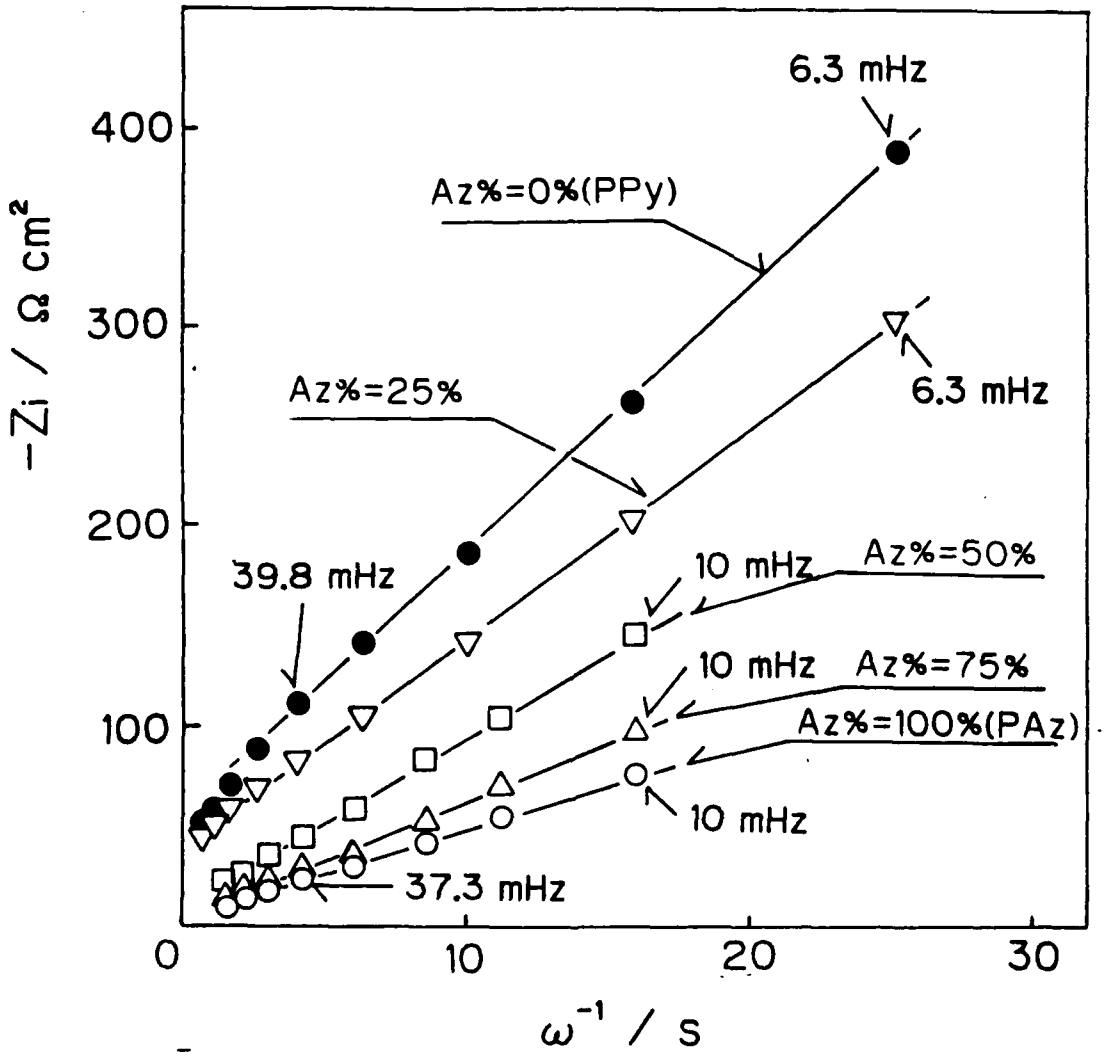
6.3 mHz
400
Az%=0%(PPy)
300
-Zi / Ω cm²
Az%=25%
6.3 mHz
200
39.8 mHz
10 mHz
Az%=50%
10 mHz
Az%=75%
Az%=100%(PAz)
100
10 mHz
37.3 mHz
0
10
20
30
ω⁻¹ / s

Fig. 6

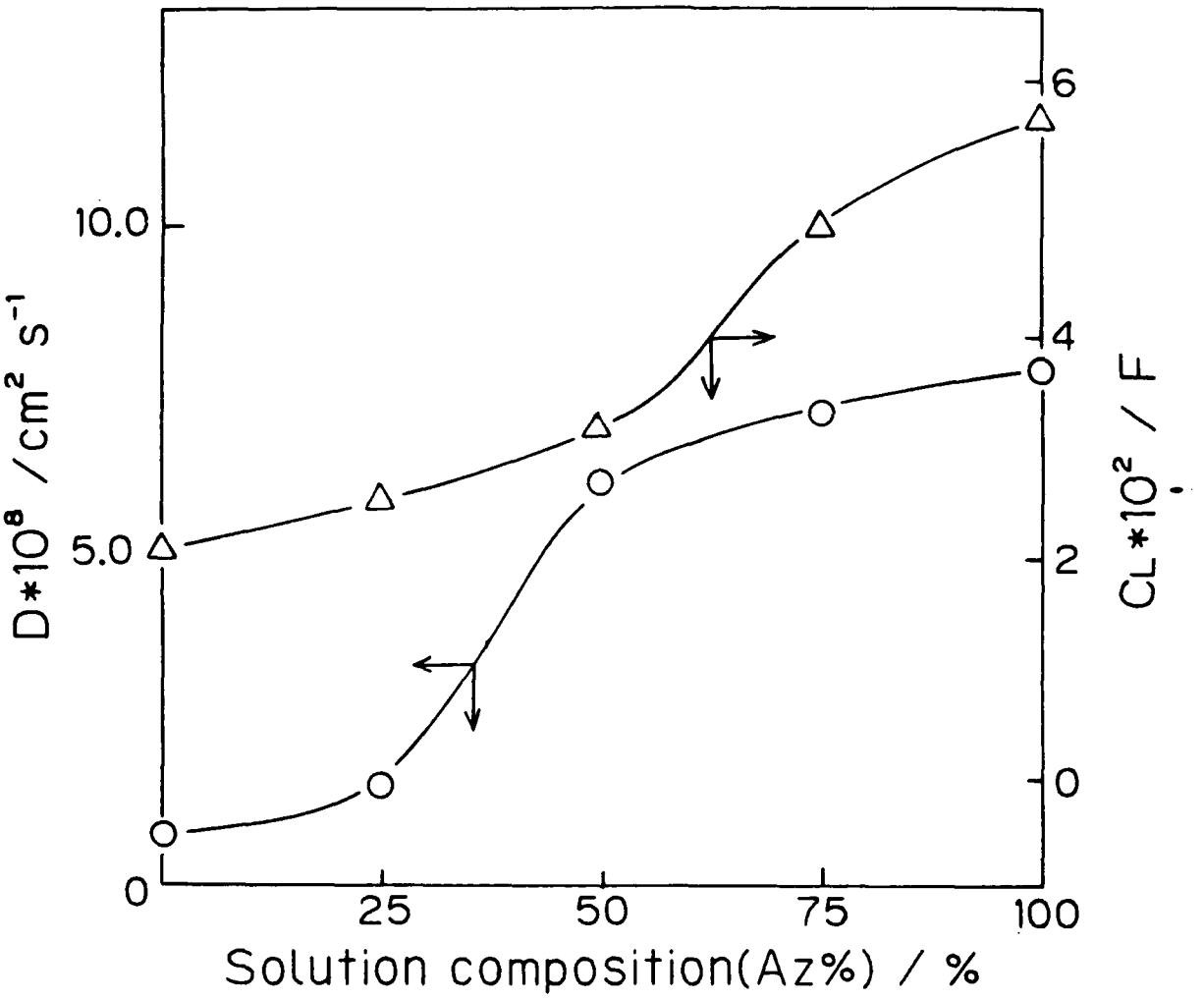
10.0
5.0
0
D*10⁸ /cm² s⁻¹
6
4
2
0
CL*10² / F
25
50
75
100
Solution composition(Az%) / %

Fig 6

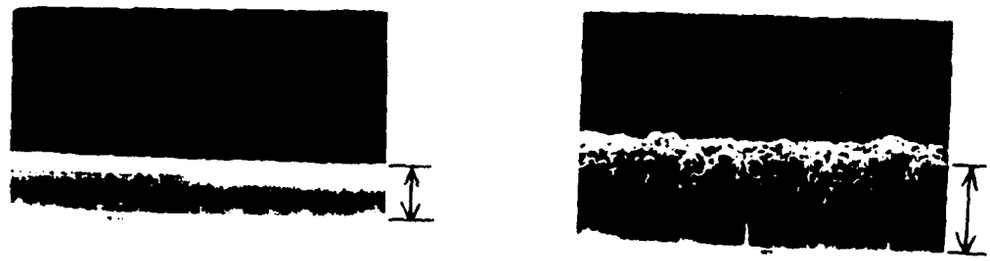

Az%=0%(PPy)

8 μm

Az% = 50 %

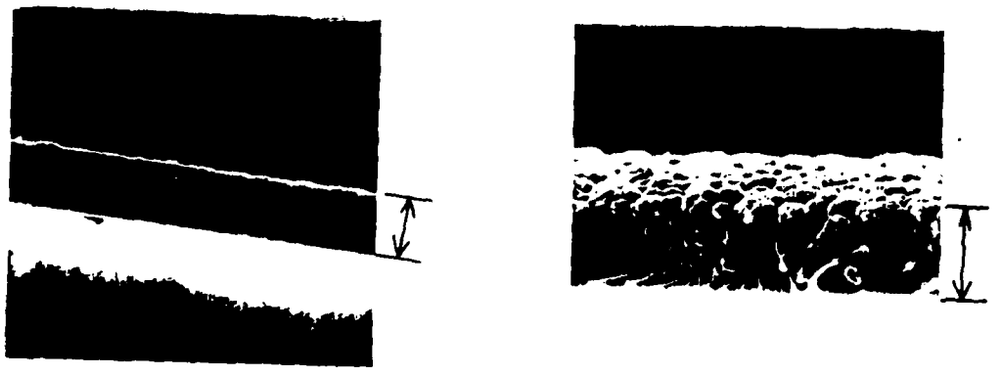

Az%=25%

Az%=100%(PAz)

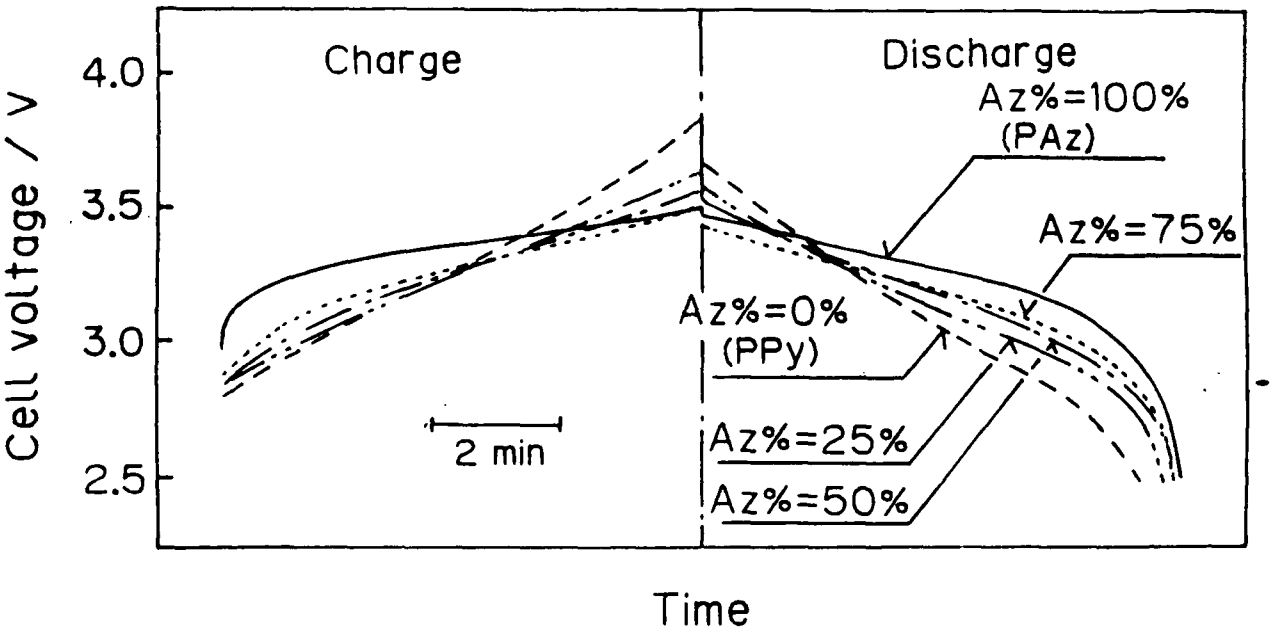
Charge
Discharge
Az%=100%
(PAz)
Az%=75%
Az%=0%
(PPy)
Az%=25%
Az%=50%
2 min
4.0
3.5
3.0
2.5
Cell voltage / V
Time

Fig 3

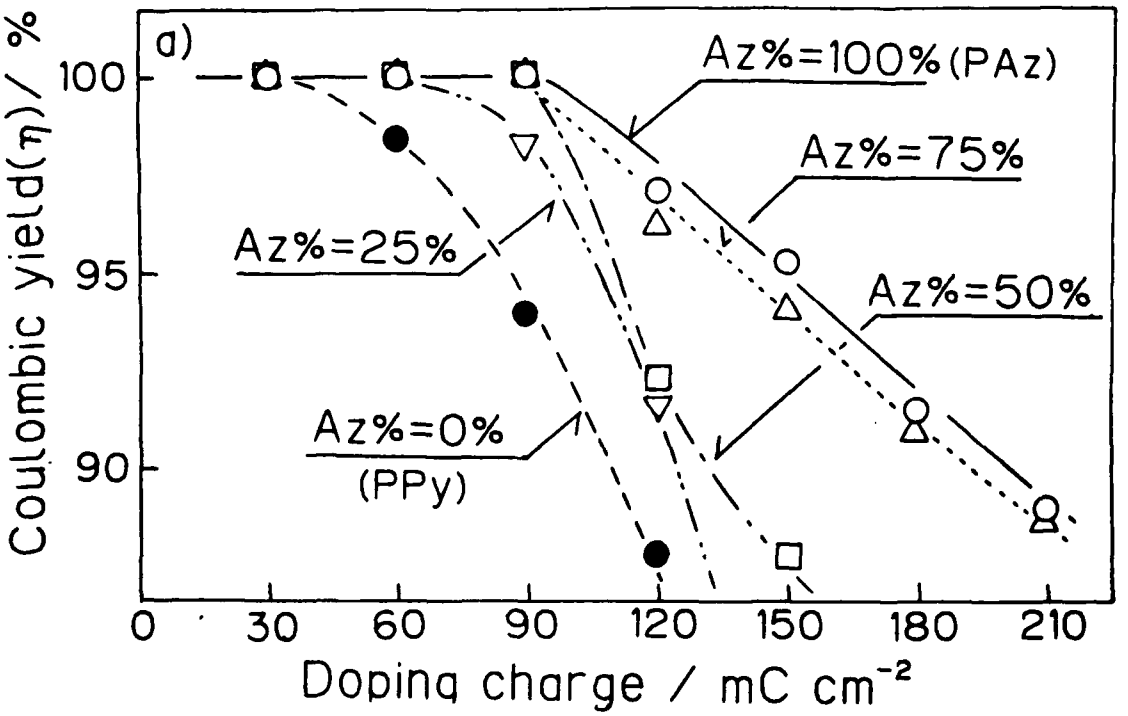
a)
Coulombic yield(η)/ %
100
95
90
Az%=100% (PAz)
Az%=75%
Az%=50%
Az%=25%
Az%=0%
(PPy)
0
30
60
90
120
150
180
210
Doping charge / mC cm⁻²

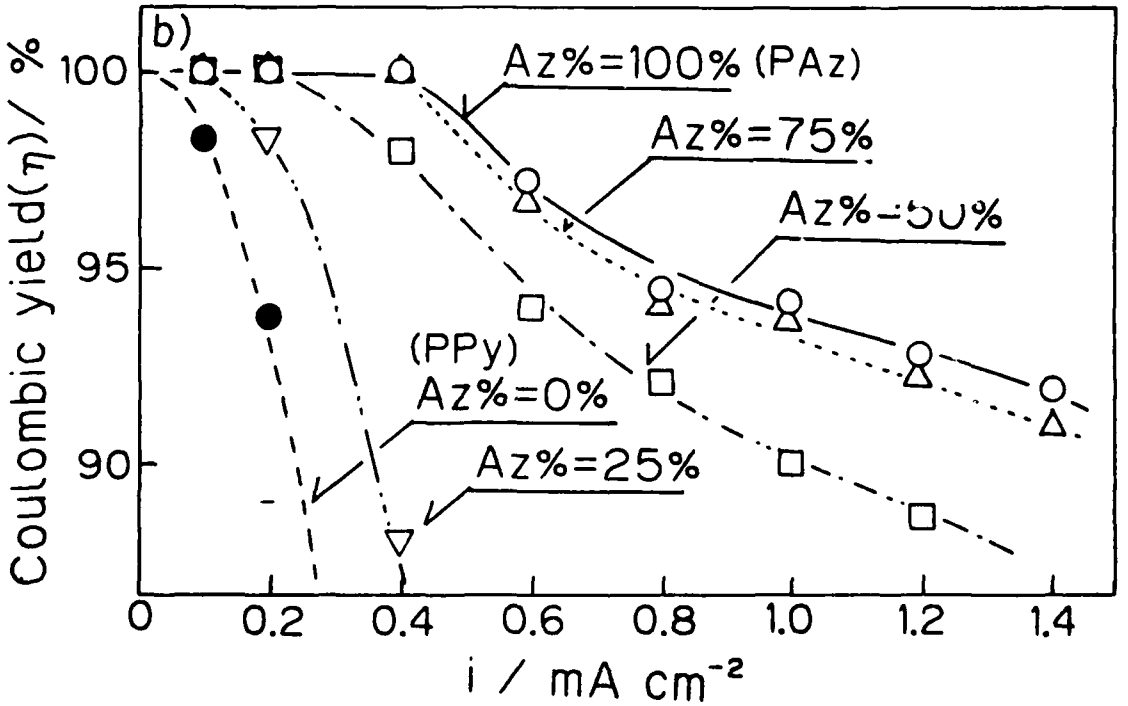
b)
Coulombic yield(η)/ %
100
95
90
Az%=100% (PAz)
Az%=75%
Az%=50%
(PPy)
Az%=0%
Az%=25%
0
0.2
0.4
0.6
0.8
1.0
1.2
1.4
i / mA cm⁻²

Fig. 1